

Seismic analysis of abutment events at LaRonde mine

Ben Ollila^{a,*}

^a SRK Consulting, Canada

Abstract

The purpose of this paper is to characterise the source mechanisms of two large seismic events (magnitude $M_{\text{Nuttli}} \geq 3.0$) using routine seismic data analysis tools. When there is no clear evidence of source mechanism type, there is a prevailing tendency to attribute fault slip mechanisms to large magnitude seismic events. This study uses seismic source parameter analysis to highlight characteristics of two large events that are more consistent with a stress-driven mechanism than a fault-related failure process.

While fault-related seismicity tends to be confined to the plane of a geologic feature, stress-driven seismicity tends to be controlled by regions of mining-induced stress around mine voids and can migrate as mining progresses. Using seismic data from an ultra-deep open stoping mine in northern Quebec, this study characterises a migrating rock mass failure region in the mine abutments. The locations of seismic events, including mine-scale occurrences, are linked to the advancing stoping front of the mine abutment.

Introducing a novel tool, plane-based time–distance charts, enables the exploration of migrating regions of rock mass yield and facilitates event clustering for source parameter analysis. The self-similarity of the large events with the broader migrating failure region is assessed using the Gutenberg–Richter frequency–magnitude relation. This analysis sheds light on the distinctive nature of stress-induced rock mass yield zones, providing insights for seismic hazard assessment in deep mining environments.

Keywords: mine seismicity, mine-scale event, seismic data analysis, underground mining

1 Introduction

In high stress mining, large seismic events remain a significant safety and financial risk, despite decades of advance in rock engineering. In the previous 15 years, numerous high magnitude seismic events, including some resulting in close calls and extensive damage, have occurred across multiple world-class operations. It is commendable when mine operators permit publication of case studies surrounding these large, damaging events, as they provide significant learnings for the mining industry. Notable examples of high profile rockbursts that caused widespread damage include a multi-year sequence of magnitude M_{Nuttli} (MN) 3.8 events at Kidd Creek mine from 2009–2011 (Counter 2014) and a more recent occurrence in 2020 moment magnitude (MW) 4.2 at Kiruna mine (Dineva et al. 2022).

Source mechanisms of high magnitude events ($M_{\text{N}} \geq 3.0$) have a prevailing tendency to be shear related and usually occur on pre-existing geologic discontinuities. Mining related seismic events of exceptionally high magnitudes tend to have exceptionally large source mechanisms. Source radius models such as the Brune model, assume a circular failure surface on a fault that is proportional to the corner frequency of the event (Brune 1970). Using these source models, it is not uncommon for the largest mining related events to have estimated source diameters greater than 100 m, or even hundreds of metres. It follows that processes involved in the generation of these large events can exist on a similar spatial scale to a large part of the mine.

In March 2005, one of the largest recorded mining related seismic events, an ML5.3, took place in the Klerksdorp district of South Africa. This event caused significant damage to surface buildings and injuries to

* Corresponding author. Email address: bollila@srk.com

over 50 people, including two fatalities. The conclusion from Durrheim et al. (2006) was that the accumulation of mining over several decades had led to the event.

Mine-scale seismic events are seismic events that are part of rock mass failure processes that exist on a similar scale to the mine or a large part of the mine. In Canadian mining, it has been suggested that MN3.0 provides an estimate to a lower end magnitude for a ‘mine-scale event.’

1.1 The problem of mine-scale events in Canada and high stress mining

The frequency of mine-scale events has sharply increased in Canada in the past decade. Events of magnitude 3.0 or greater are of sufficient size that they are usually recorded by the national seismic system, therefore a near complete dataset exists of large mining events in Canada since 1985. The Earthquakes Canada recorded magnitude scale in eastern Canada is MN. Figure 1 shows the yearly total of MN ≥ 3.0 recorded by Earthquakes Canada per year.

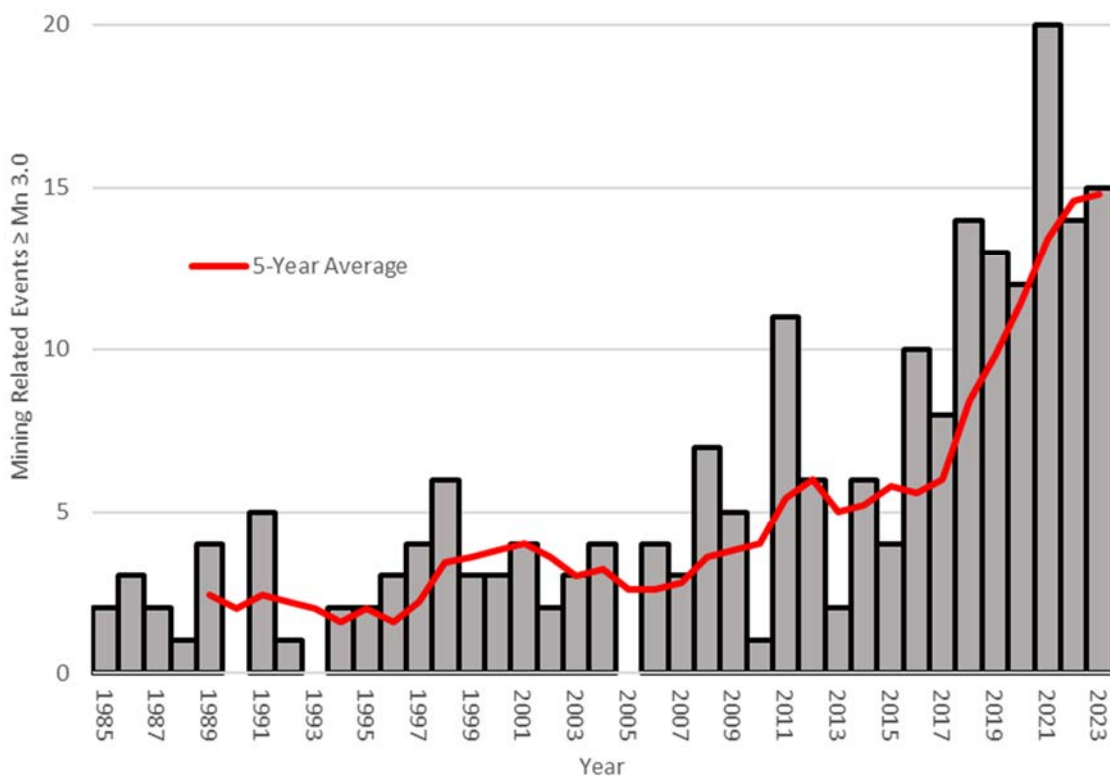


Figure 1 Mining related events MN ≥ 3.0 per year in Canada (data from Earthquakes Canada 2024)

The historical average of mine-scale events from 1985 to 2009 was 3–4 per year across the entire Canadian mining industry, but the previous decade has seen a drastic increase, with at least 12 occurrences per year in the past six years.

Factors for the increased frequency of large events likely include the high level of maturity of many Canadian operations as well as the tendency for deeper and higher stress extraction. Eighteen different mines in Canada have had events greater than magnitude 3.0 since 2009. Seventeen of these mines are still operating, and 10 have had multiple events of this magnitude. It should be noted that out of the top four mines with the most recorded events MN ≥ 3.0, three are the deepest mines in Canada. Revealingly, the greatest magnitudes since 2009 have also occurred at these mines. LaRonde and Kidd Creek are now mining below 3,000 m depth, and Creighton is mining below 2,500 m.

1.2 Understanding source mechanisms of mine-scale events

Hedley (1992) suggested that rock mass failure processes involved in mining related seismic events can be broadly classified as volumetric failure or contact failure. Volumetric failure can be best described as rock mass fracturing in a three-dimensional volume, while contact failure tends to occur on a pre-existing planar weakness, such as a fault.

Source mechanisms of mine-scale events are generally thought to have a tendency to be shear related, usually occurring on faults. South African experience from Western Deep Levels, reported by Lenhardt (1988), indicated that over 80% of events greater than MW3.0 were related to slip on pre-existing discontinuities, with a subset (20%) being related to slip in high stress abutments and pillars. Fifteen percent were related to pillar failure and a small minority (5%) were recorded as ‘abutment events.’

Ortlepp & Stacey (1994) suggested approximate magnitude bounds on source mechanism, with only shear rupture (Ortlepp Shears) and fault slip having maximum magnitudes (Richter) greater than 3.0.

The previously mentioned 2020 MW4.2 at Kiruna was likely related to a regional pillar, caused by a low extraction area between two highly extracted areas, but the specific mode of failure was complex (Dineva et al. 2022). It is notable that large seismic events often can have ambiguous failure mechanisms and can occur at unexpected times.

When a mine-scale event occurs, it is desirable that the following be understood:

- Time – why did the event occur at its time?
- Location – why did the event occur at its location?
- Magnitude – what contributed to the source size and energy release of the event?

Back-analysis of seismic data, site characterisation of geology and structures, underground observations of deformation prior to and after large events, as well as numerical modelling are all key components of understanding the occurrence of large events. Moment tensor inversion can provide insight into the forces involved in an event, as well as potential fracture planes. Numerical modelling is useful to understand potential distributions of stress and strain that may be influential in mine-scale events. Comparison of blast data and seismic data can yield insights into patterns between seismogenic rock mass failure processes and mining-induced stress change.

A critical component of a back-analysis of a large event is to understand the seismogenic rock mass failure process around (prior to and after) the large event. This is done through analysis of the surrounding seismicity in space and time, including foreshocks and aftershocks, to gain understanding of the rock mass failure processes involved in and affected by the rupture. For a mine-scale rock mass failure process, it is not always clear what spatial and temporal bounds to place on surrounding data, and separate insights may be gained from assessing multiple spatial and temporal scales (Ollila 2021).

2 LaRonde mine

2.1 Background

The remainder of this paper will focus on an analysis of large events occurring in the abutment of Canada’s deepest gold mine, Agnico Eagle’s LaRonde mine. The LaRonde orebody is a gold-bearing volcanogenic massive sulphide deposit, located in the Abitibi greenstone belt. LaRonde uses transverse primary-secondary longhole open stoping at depths greater than 3,000 m below surface. Figure 2 shows an image of historic, current and planned mining at LaRonde mine.

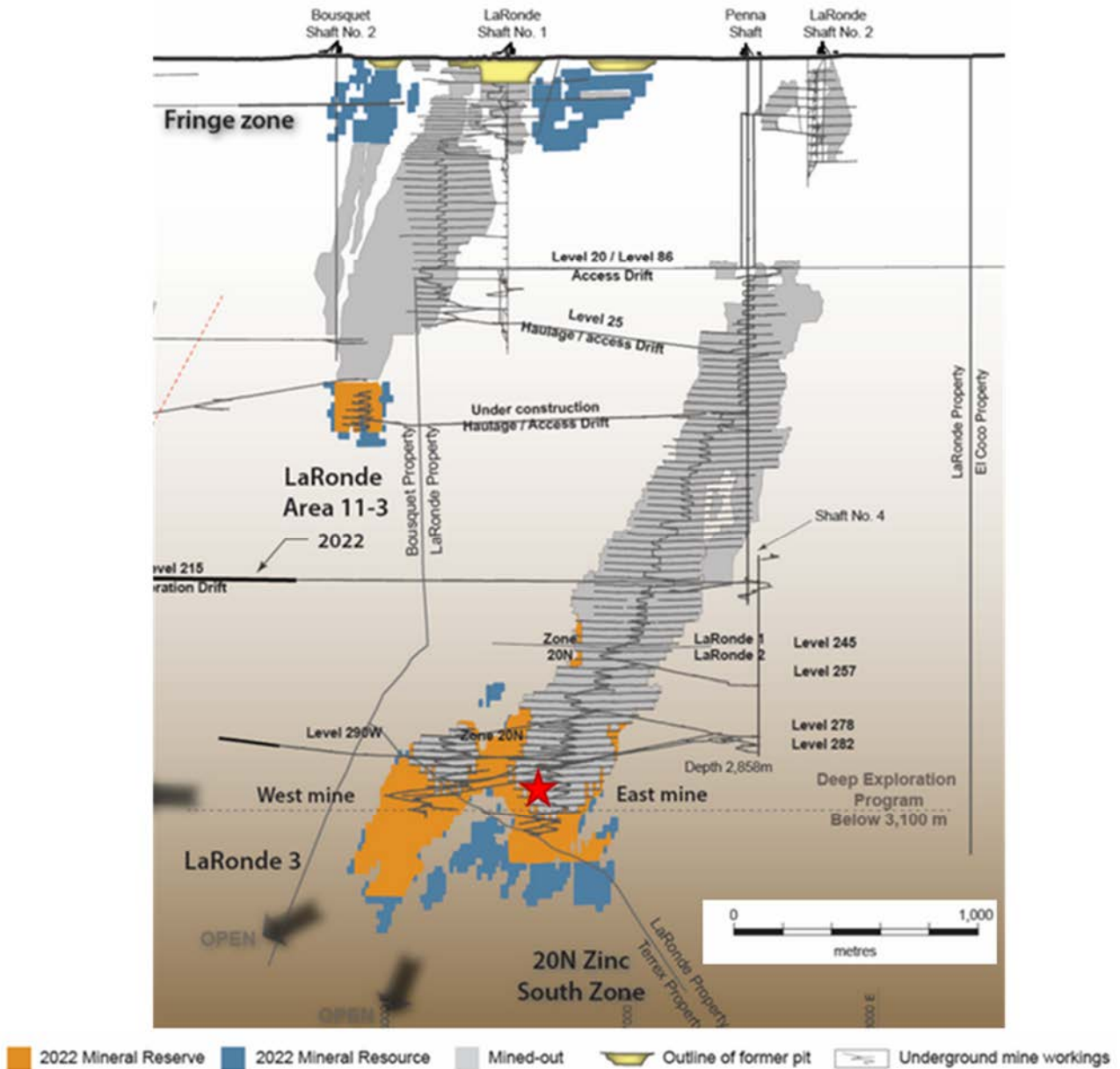


Figure 2 LaRonde mine, with area of study shown by red star (modified from Agnico Eagle 2024)

Anisotropy at LaRonde has a significant influence on rock mass strength. It has been noted that a steeply dipping foliation has a significant impact on tunnel stability, depending on the angle of incidence between the excavation boundary and foliation orientation (Turcotte 2010).

The Zone 20 North deep extension at LaRonde mine employed a diamond-shaped stope sequence; expanding in overhand, underhand and lateral chevrons that are designed to shed stress to the abutments, as described by Mercier-Langevin (2010). The seismic events studied in this paper are on the west abutment of the east mine, as designated by the star in Figure 2.

2.2 Seismicity at LaRonde mine

Due to the great depth of mining (3,000 m+) at LaRonde, the seismic hazard is high relative to other Canadian mines. In the previous 15 years, LaRonde has recorded more $MN \geq 3.0$ than any other mining operation in Canada. Since recording its first event $MN \geq 3.0$ in 2007, LaRonde has recorded nearly 70 events to date, including a $MN4.5$ event in 2024.

Heal et al. (2005), Hudyma & Brummer (2006) and Mercier-Langevin (2010) reported that seismic events in the vicinity of the mine abutment tended to migrate with stoping, interpreted as a stress-induced failure zone in the Zone 20 orebody at LaRonde. Section 3 consists of an examination of similarly behaving abutment events in the lower abutment of the mine, specifically to assess the link between the abutment failure region and two $MN \geq 3.0$ events.

3 Abutment mine-scale events at LaRonde

1.1 Seismic data

The seismic events of interest for this case study are two that occurred in the lower west abutment of the Zone 20 orebody between August 2018 and January 2019. Source parameters for these events are shown in Table 1.

Table 1 Source parameters for large events as recorded by the LaRonde mine seismic system

Date	MW	MR	MN	Moment (Nm)	Energy (J)	Residual (m)	Max. disp. (mm)	Es:Ep	Source radius (m)
2018-08-19	2.3	3.0	3.1	3.1E+12	4.2E+07	4.7	22	14	52
2019-01-14	2.2	3.1	3.2	2.3E+12	1.0E+08	3.9	20	17	36

Three magnitudes are listed for the events:

1. Moment magnitude (MW), as recorded by the mine seismic system.
2. Richter magnitude (MR), recorded by the Regional Seismic Network (Wesseloo et al. 2011).
3. Nuttli magnitude (MN), recorded by Natural Resources Canada (2024).

Additional source parameters listed are recorded by the mine seismic system.

Forty-one months of data surrounding the large events were included for analysis in order to establish the behaviour of seismogenic rock mass failure processes prior to and after the large events.

3.1 Visualisation of foreshocks and aftershocks

After the occurrence of a large event, insights into the source mechanism can often be gained by assessing the location of the aftershocks. Foreshocks, or events occurring as in the leadup to the mainshock, can be more difficult to analyse in seismic sequences due to their relative infrequency in comparison to aftershocks (Utsu 2002; Kagan & Knopoff 1976). Aftershocks are the result of the large stress change from the mainshock and typically occur at the greatest frequency nearest in time to the main shock. The frequency tends to decrease over time after the mainshock (Omori 1894). Foreshocks, however, do not tend to have regular behaviour and mainshock source locations can be active or inactive prior to the mainshock. Additionally, difficulty arises in mine seismicity when events are caused by multiple source mechanisms simultaneously, with multiple failure mechanisms potentially adding confusion to the study of the source mechanism (Hudyma 2008).

Following a substantial seismic event, stress within the rock mass is redistributed both statically and dynamically. Aftershocks are believed to stem from the redistribution of strain energy, initiating subsequent smaller seismic occurrences (Stein 1999).

In Maeda's (1999) view, two potential connections between foreshocks and a significant event are identified:

1. Foreshocks may indicate a broader escalation in stress within the area, subsequently leading to the main shock.

- The presence of foreshocks could redistribute stress to the region, eventually culminating in the main shock.

Separate seismic populations were observed to exist in the hanging wall and footwall of the abutment, and these were assessed separately. One month of foreshocks and one month of aftershocks for both hanging wall and footwall events are visualised in Figure .

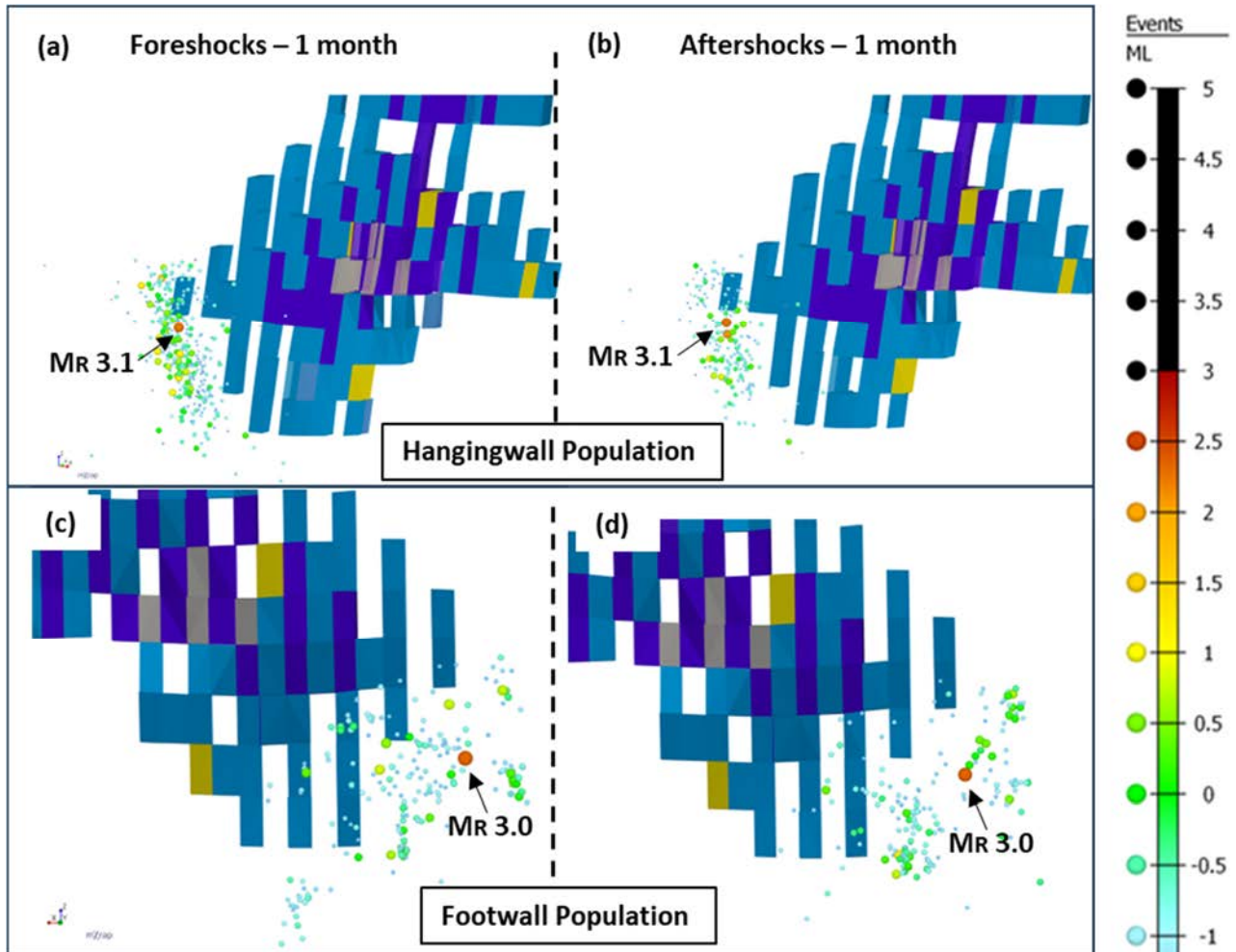


Figure 3 (a and c) Foreshocks and (b and d) aftershocks to the large events in the hanging wall population and footwall population

For Figure 3, the large events are observed to fit within the main cluster of seismicity, potentially indicating they are generated by similar source mechanisms. There is little difference between the location of foreshocks and aftershocks of the hanging wall event, both of which tend to align along the lower stopping front. Aftershocks of the footwall event, however, appear to locate further into the abutment than the foreshocks.

3.2 Visualisation by date

To establish trends and relations between microseismicity and mining, it is desirable that seismic data be available, high quality and consistent for the entire duration of potentially influential mining. In order to analyse long-term trends in microseismicity around the event of interest at LaRonde, multiple years of seismic data were necessary to establish large-scale trends. Event clusters nearby the large events were separated by the hanging wall and the footwall. Figure 4 shows the events coloured by relative date.

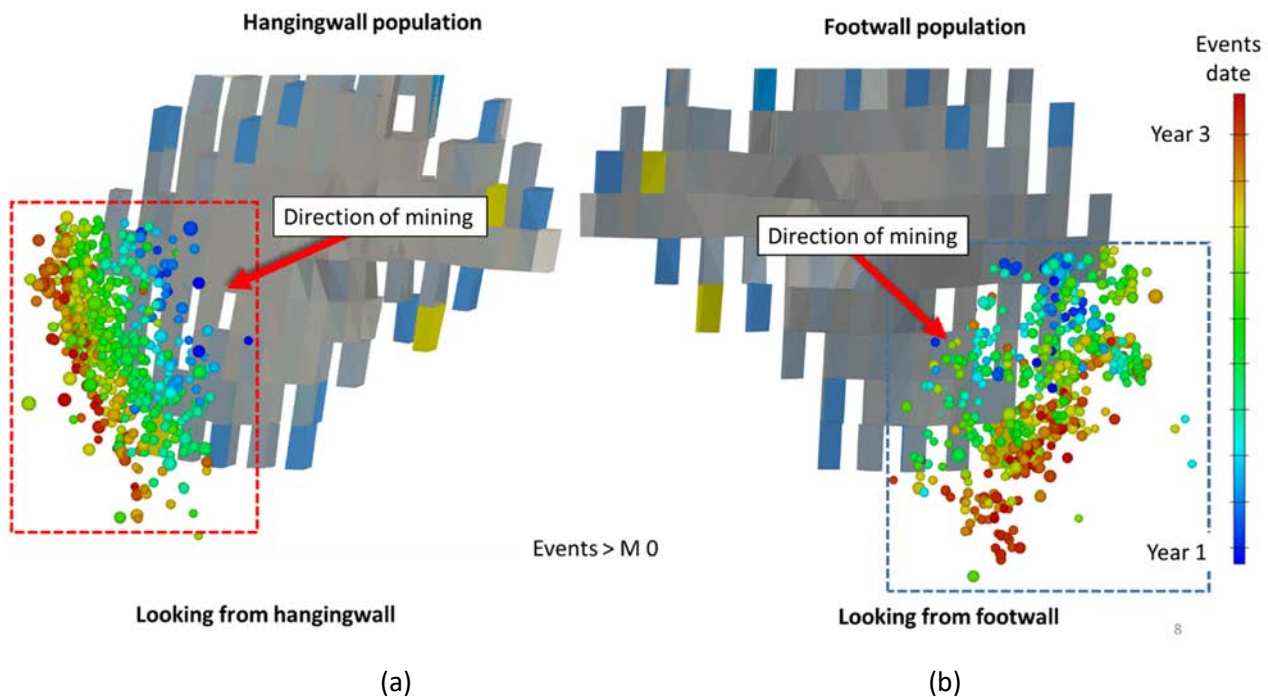


Figure 4 Events $MW \geq 0$ coloured by date in the (a) hanging wall and (b) footwall

Colouring events by date effectively shows two migrating seismogenic regions, one in the footwall) and one in the hanging wall. Two populations of seismicity over a three-year time period can be observed to migrate parallel to the direction of mining.

The event colour distribution tends to take a semi-planar form, which is a feature sometimes associated with a fault slip mechanism. The direction of migration of the seismogenic population, however, is observed to be perpendicular to the planar shape, which is inconsistent with a fault-related mechanism.

3.3 Time–distance analysis

Seismic events tend to cluster in space and time based on the seismic source mechanism (Hudyma et al. 2003). The purpose of time–distance analysis (TDA) charts is to simplify assessment of the migration of seismic clusters. TDA is a clustering technique that simplifies the time-space domain to a time–distance domain by transforming event location to a distance from a location of interest. Ollila (2021) used TDA to identify coalescence of seismicity around the hypocenter of a mine-scale event at Nickel Rim South mine, attributing the source mechanism to fault asperity like behaviour. Somewhat similarly to this study, Abolfazlzadeh (2016) tracked the median elevation of a seismogenic zone above a cave at Telfer mine over time and assessed source parameter variation across the seismogenic zone.

To assess the abutment event population as a migrating seismogenic zone, investigation of the following aspects was completed:

- Analysis of the travel distance and rate of movement of the seismogenic zone.
- Comparison between locations of seismic hypocentres and blast locations.
- Comparison of source parameters across the seismogenic zone.

3.3.1 Time–distance analysis formulation

Figure 5 illustrates a 3D visualisation of the time–distance chart.

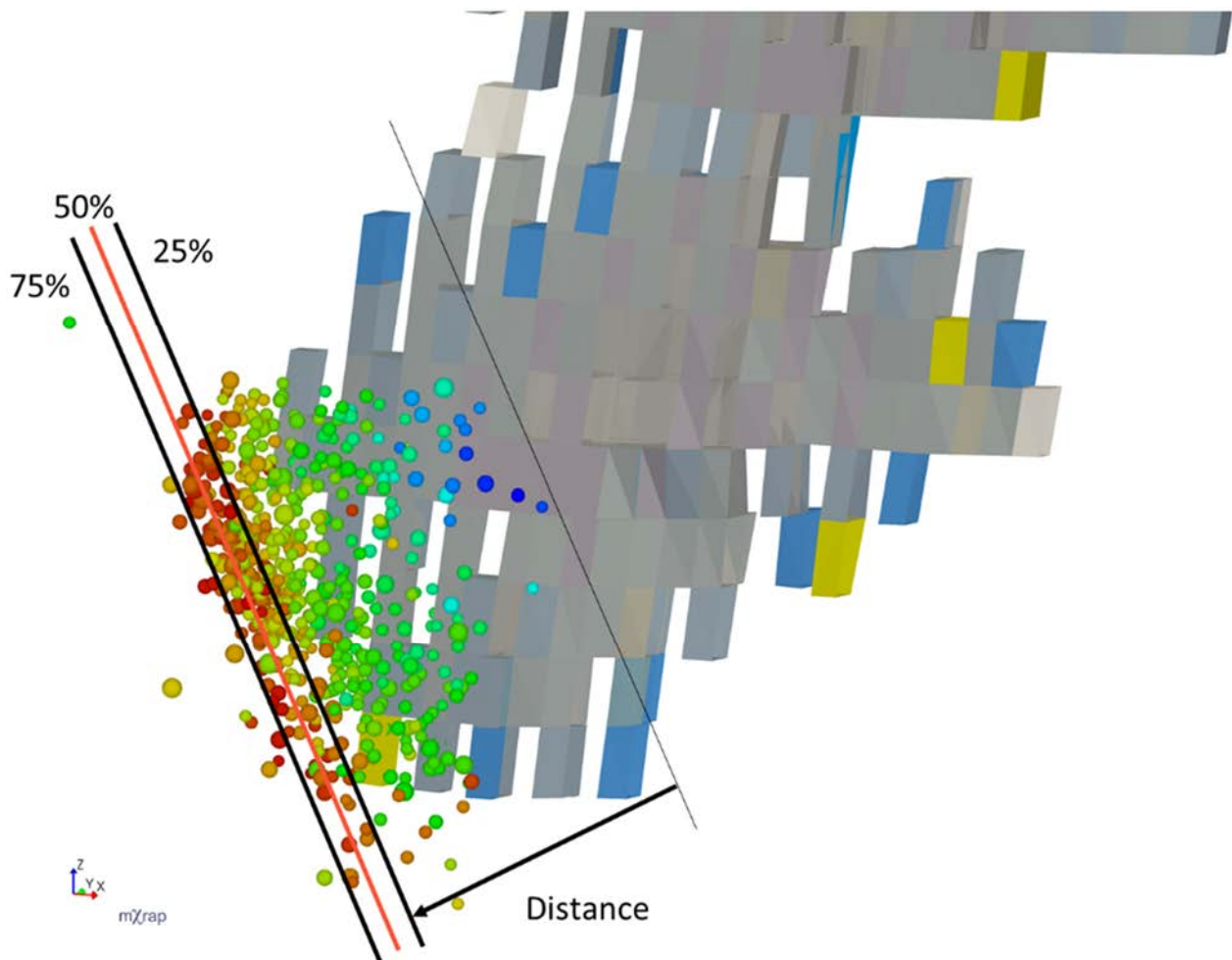


Figure 5 Visualisation of percentile distance of hanging wall events to a base plane

The time–distance chart used for this case study calculates the normal distance from each event to a plane oriented parallel to the seismogenic zone and placed at the centre of the diamond-shaped mining sequence. The migration of seismic events could then be tracked using the 25th percentile, median and 75th percentile distances from the base plane.

3.3.2 Plane fit

To approximate the orientation of the seismic populations, principal component analysis was performed using the plane-fitting *mXrap* application (Harris & Cumming-Potvin 2023). In order to approximate the sub-planar seismic population, seismic events occurring in a two-month span after the main shocks were used to approximate parallel planes to the footwall failure region and the hanging wall failure region (Table 2).

Table 2 Best-fit plane

	Dip	Dip direction	Fit quality
Hanging wall event aftershocks	75	50	Good
Footwall event aftershocks	50	100	Moderate

3.3.3 Time–distance chart for footwall seismogenic zone

A time–distance chart of the seismogenic zone in the footwall is shown in Figure 6.

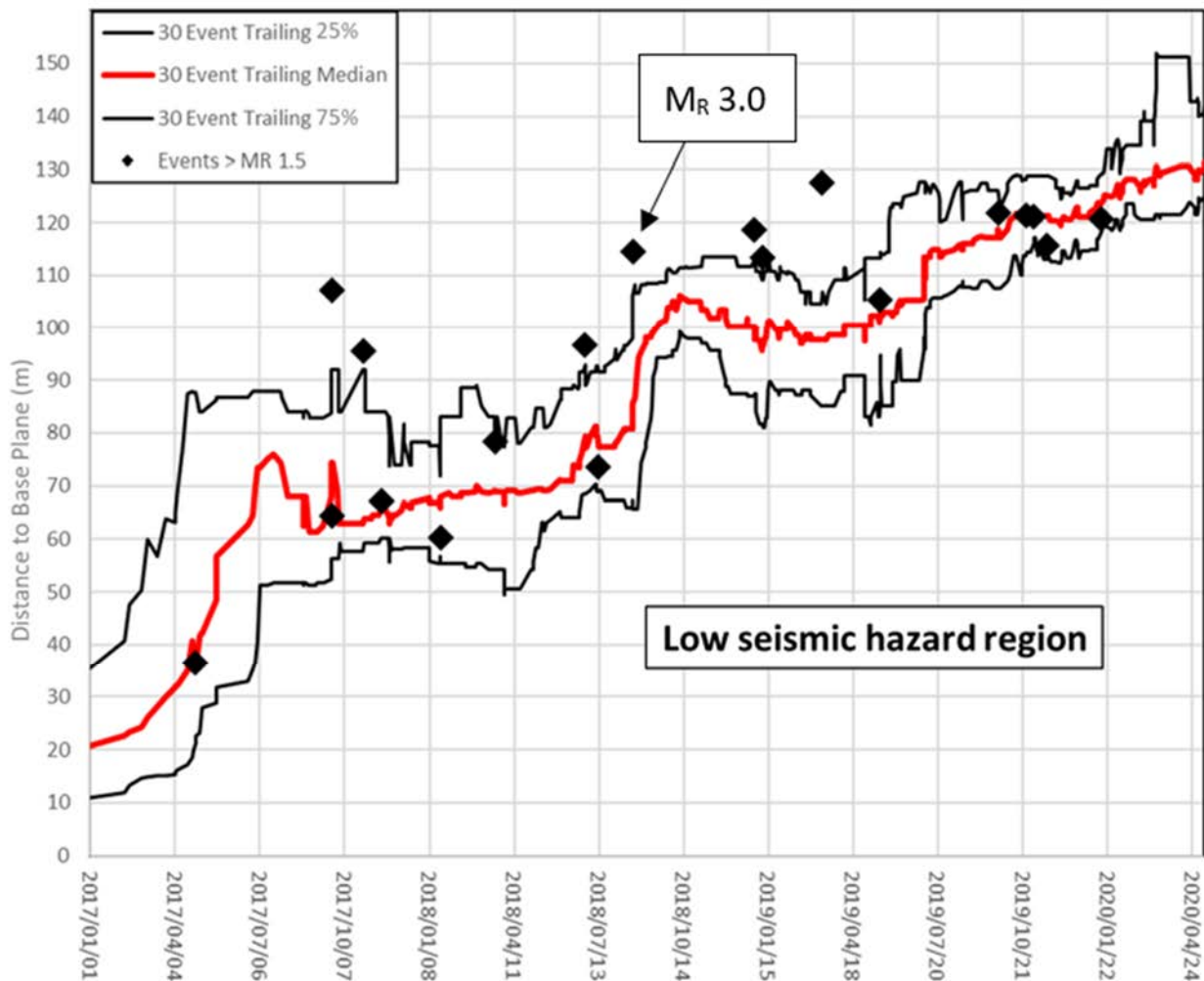


Figure 6 Time–distance chart of footwall seismic population

A 30-event trailing period was used to calculate the 25th, median and 75th percentile distances to the base plane in order to approximate the movement of the seismogenic zone. It can be observed that the event median line migrates 110 m over the 40-month monitoring period. The rate of movement and the width of the seismogenic zone becomes more consistent with time.

Over the monitoring period, all events greater than MR1.5 took place within or just ahead of the seismogenic zone. This shows that the location of the seismogenic zone is important to designate regions of high seismic hazard within or ahead of the seismogenic zone, and lower seismic hazard behind the seismogenic zone.

The August 2019 MR3.0 locates just ahead of the 75-percentile line, conceivably fitting with the location of the seismogenic zone. After the large event occurs, the seismogenic zone ‘jumps’ ahead approximately 25 m. The resultant movement of the seismogenic zone, apparently due to the large event, is additional confirmation that the event mechanism is related to the seismogenic zone.

3.3.4 Time–distance chart for hanging wall seismogenic zone

Similarly to the footwall seismic zone, a time–distance chart for the hanging wall population using the hanging wall base plane shows a similar migrating population (Figure 7).

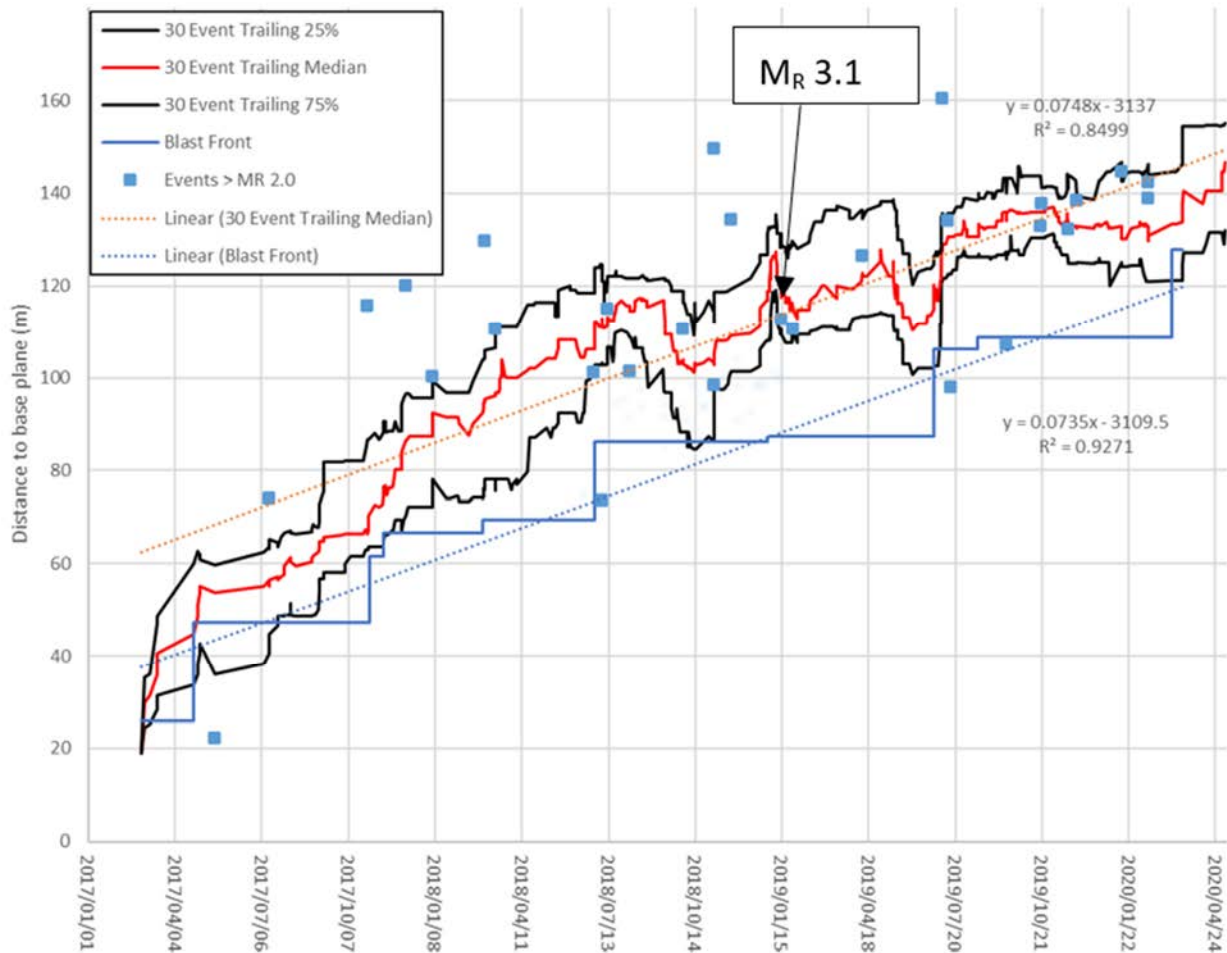


Figure 7 Time–distance chart showing a comparison between event and stope blast locations

The location of the blast centroids on the leading edge of the blast front have been added to the chart. Distance to the blast front from the base plane was calculated. A comparison between the linear trendline of the blast dataset and seismic dataset shows near identical rates of movement, indicating that blast locations control the movement of the seismogenic zone.

Twenty-nine events greater than MR2.0 appear to migrate with the seismogenic zone, shown by blue squares. Only 14% (4 out of 29) are behind the twenty-fifth percentile line, again indicating that the migration of the seismogenic zone controls the location of greatest seismic hazard. Similarly to the footwall, the location of the largest event (MR3.1) fits near to the centre of the seismogenic zone.

In comparison to the footwall seismogenic zone, the movement of the hanging wall zone is more consistent, with a tendency towards a regular width. There was no tunnel development in the hanging wall, while the footwall contains transverse crosscuts to access the stopes. It is possible that the less uniform behaviour of the seismogenic zone in the footwall was impacted by the existence of development.

3.4 Gutenberg-Richter frequency–magnitude relation

A power law has been observed to exist between the frequency and magnitude of populations of seismicity Gutenberg & Richter (1944). This relation can provide insights into source mechanisms of seismicity (Legge & Spottiswoode 1987; Hudyma 2008) as well as variations in seismic hazard (Wesseloo 2014).

3.4.1 Self-similarity of the large events with abutment seismogenic zones

The frequency–magnitude relation can be used to demonstrate the self-similarity of a seismic population. While the frequency–magnitude relation of a population is linear, a population is said to be self-similar, while bimodal behaviour can be caused by combined populations of separate source mechanisms (Amidzic 2001). Lack of fit between a large event and other events from a population decreases the confidence that the events are part of the same rock mass failure process.

Richter magnitude, as recorded by the regional seismic network (RSN), was used to assess the self-similarity of the hanging wall and footwall populations. The RSN is a local seismic network that is designed to record a magnitude range that is too large for the mine seismic system to record accurately and too small for the national seismic system (Earthquakes Canada) to record all but the largest events (Wesseloo et al. 2011). The RSN Richter magnitude is correlated with the time and location of large seismic events recorded by the mine.

Gutenberg–Richter frequency–magnitude (GRFM) charts for both footwall and hanging wall populations are shown in Figure 8.

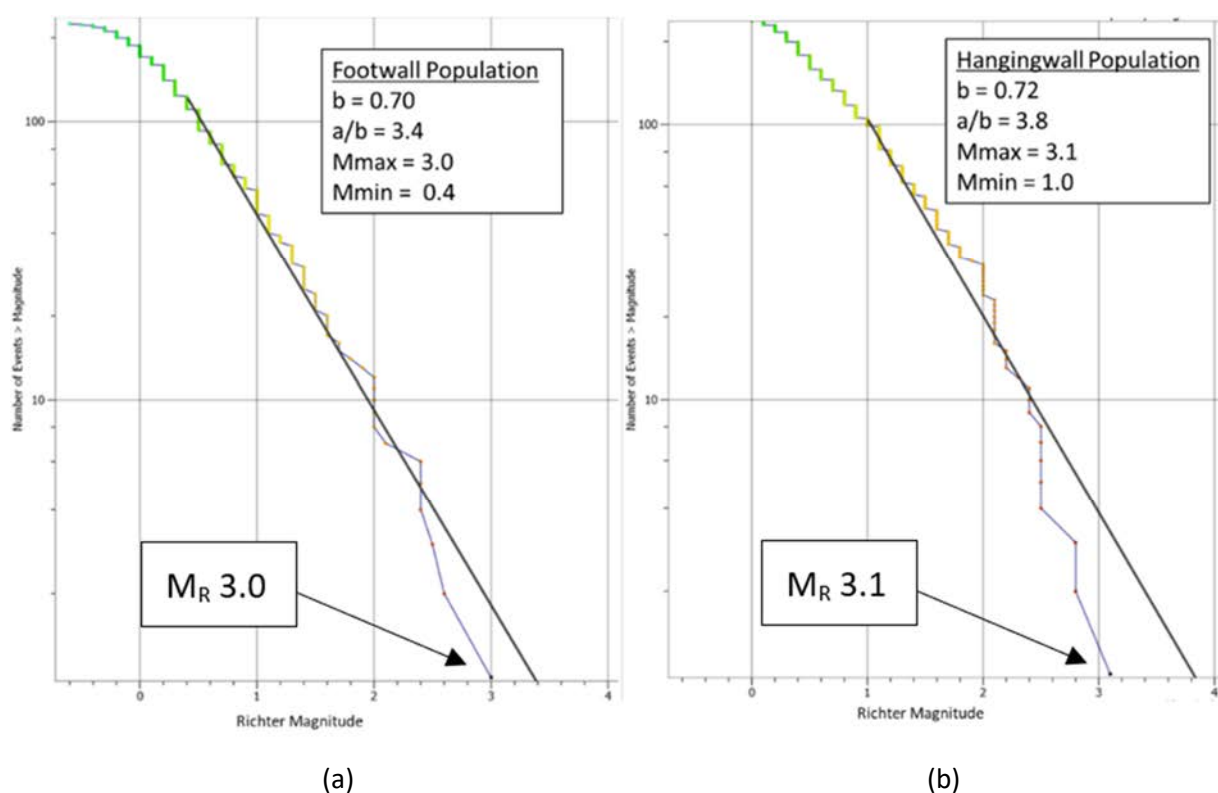


Figure 8 Regional seismic network frequency–magnitude relation for monitoring period for the (a) footwall population and (b) hanging wall population

Although the sizes of the datasets are too small to make reliable conclusions, it is notable that the magnitude of the large events is consistent with others in the dataset, which supports the hypothesis that these large events are part of the same source mechanism as the rest of the events in the seismogenic zone.

3.4.2 Seismic hazard variation in footwall population

Part of the utility of the time–distance charts is that it allows the seismogenic population to be subdivided for source parameter analysis based on relative-distance from the base plane. Therefore, source parameters on the leading edge of the seismogenic zone can be compared to those on the trailing edge. For the purposes of this investigation, the seismogenic zone was divided into quarters based on percentile distance.

GRFM charts for each quarter of the population were used to compare the spatial variation in seismic hazard across the seismogenic zone (Figure 9).

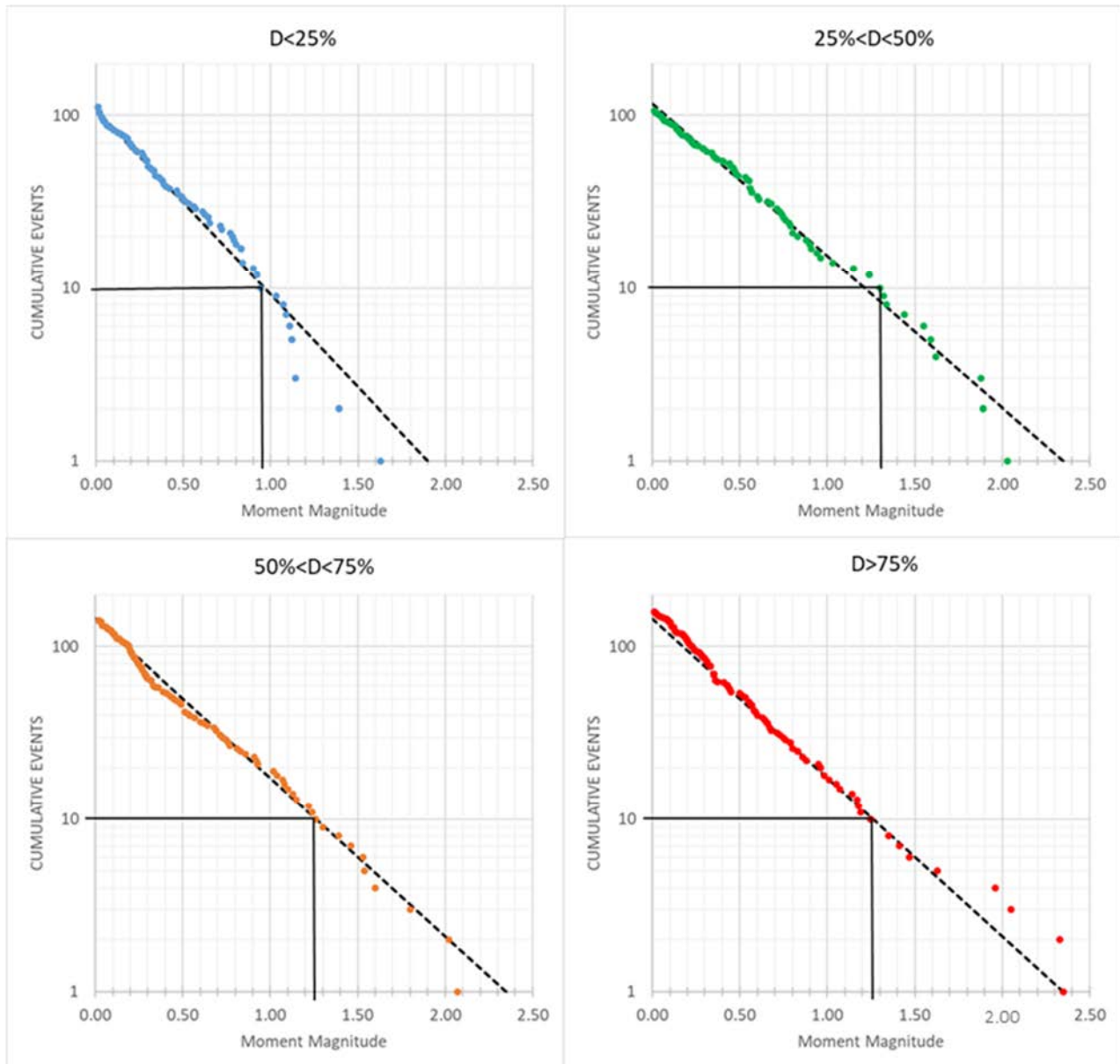


Figure 9 Gutenberg–Richter frequency–magnitude charts for each quarter of the footwall population

The quarter-populations were just over 100 events each, and the largest events tended to deviate from the linearity of the best-fit line at the highest magnitudes. In order to compare seismic hazard between the seismic populations, the 10th largest event was compared, since all populations had a relatively linear fit at this magnitude range. While the leading three quarters ($D \geq 25\%$) of seismogenic zone have a similar magnitude ($MW 1.3$), the trailing quarter ($D < 25\%$) has a lower magnitude ($MW 0.95$), indicative of a higher seismic hazard in the leading 75% of the seismogenic zone, and a lower seismic hazard in the lagging 25% of events.

A consistent but weaker variation in seismic hazard was observed across the hanging wall seismogenic zone.

3.5 Apparent stress

The apparent stress of a seismic event is an estimate of the stress release associated with the event (Boatwright 1984). Variations in apparent stress have been used to infer source regions of higher or lower relative stress (Van Aswegen & Butler 1993).

In order to study variations in apparent stress across the seismogenic zone, cumulative distributions of apparent stress for different regions of the seismogenic zone are shown in Figure 10.

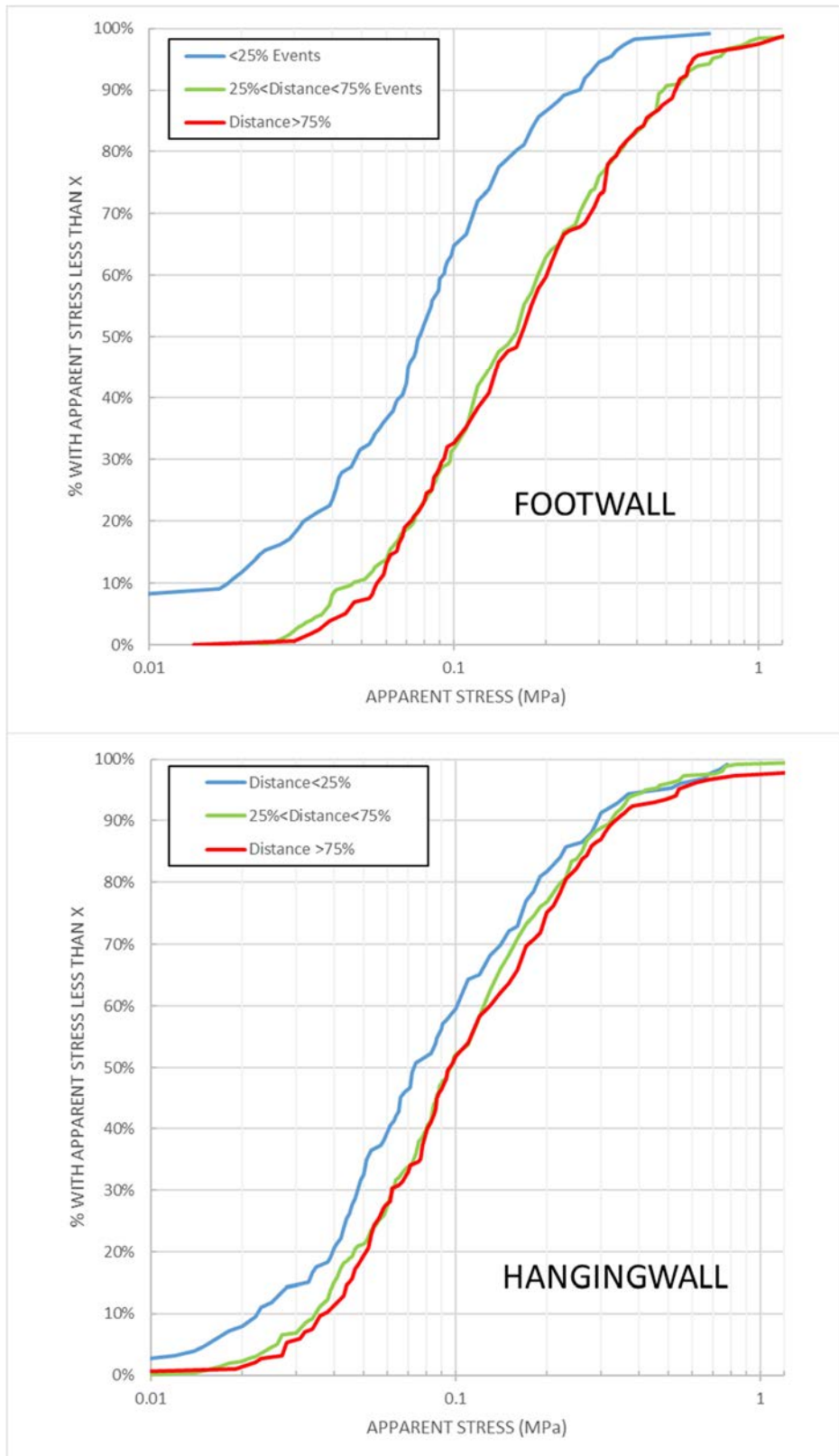


Figure 10 Cumulative apparent stress differentiated by relative distance within the footwall and hanging wall seismogenic zones

The trailing 25% of events behind the seismogenic zone, shown by the blue line, tend to have lower apparent stress than seismic events in rest of the abutment population. This finding is consistent with events occurring directly in the abutment locating in a higher stress region with those behind the mining front occurring in stress shadowed and/or yielded rock.

The footwall population tends to have a greater variation in apparent stress between the 25-percentile events and the seismogenic zone than the hanging wall population. It is possible that this variation is related to lower seismic system coverage in the mine hanging wall since most sensors are located in the footwall.

3.6 Energy–moment relationship

The variations in energy and moment have been used to infer the state of relative stress at the event hypocenter. The amount of radiated energy tends to be related to the velocity of the rupture (Mendecki 1993), while seismic moment tends to be related to the size and displacement of the rupture (Aki 1966). There is substantial variation in radiated energy for events of a given moment, with greater radiated energy being associated with a relatively higher stress source location and lower radiated energy being associated with a relatively lower stress source (Van Aswegen & Butler 1993).

Figure 11 shows that the energy–moment relation for events at distances less than the 25-percentile in comparison to the entire footwall population.

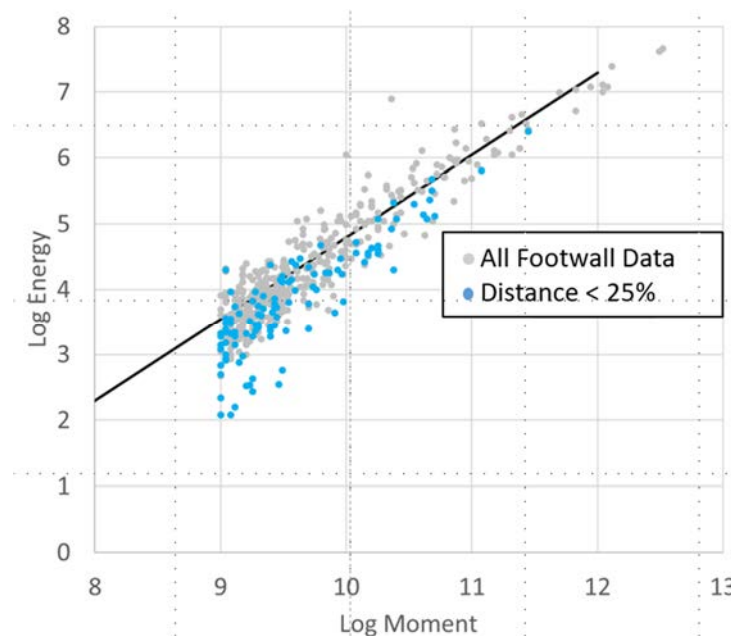


Figure 11 Energy–moment relation for footwall population with line of best-fit

It can be observed that the events behind the seismogenic zone (blue dots) tend to have lower values of moment and energy than the rest of the population (grey dots). There is a tendency for these seismic events of similar moment to have lower relative radiated energy, interpreted as resulting from greater strain occurring at lower stress, which is consistent with yielding or lower confinement.

The hanging wall seismogenic population did show a similar, but significantly weaker trend in the energy–moment relation.

4 Discussion

The primary significance of this analysis is the designation of regions of high and low seismic hazard associated with the seismogenic zones. Regions behind the seismogenic zones tend to have a lower associated seismic hazard, while the region within and ahead of seismogenic zones have a much greater seismic hazard as visualised in Figure 12.

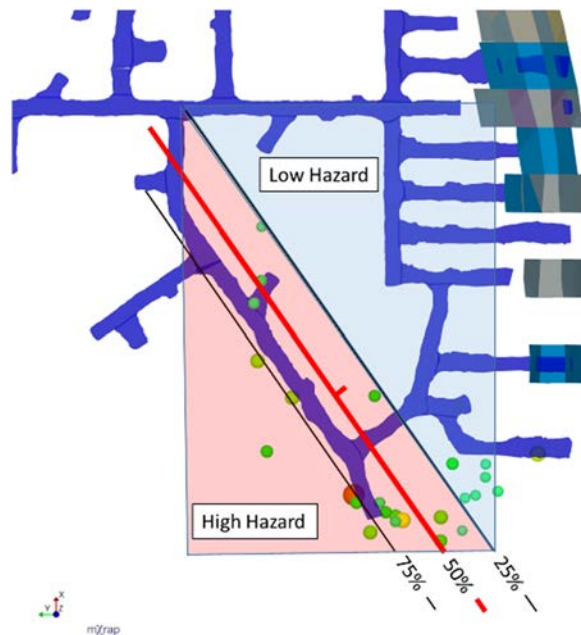


Figure 12 Designation of high and low hazard regions

Practical implications of these findings could be the improvement of seismic exclusion zones to limit exposure of personnel to high hazard areas.

Of additional significance is the inference of the source mechanism of the large events to a stress-related mechanism. While events of high magnitudes have a prevailing tendency to be controlled by locations of geologic discontinuities, the large events in this case study appear to be more likely related to the geometry of the mining front than a fault. Although the seismogenic zone is semi-planar, the direction of movement is perpendicular to the plane, which is inconsistent with a typical fault-related seismic source mechanism. This type of stress-driven seismic source mechanism for events of these magnitudes are uncommon in Canadian mining, but may be plausible at the great depths and high stresses experienced at LaRonde.

The type of fracturing that occurs in the seismogenic zone is an exceptionally interesting topic and would benefit from further research. The well developed, steeply dipping foliation is pervasive at LaRonde, and it is unknown to what degree it influences the seismogenic zone. It is possible that seismic events may at least partially take place along pre-existing foliation planes, or alternatively form fractures that crosscut the foliation.

In order to recognise the failure process related to a mine-scale event, it has been demonstrated that the related failure process to the event should be thought of on similar spatial and temporal scales to a large part of the mine. Forty-one months of data was useful to establish the patterns of the rock mass failure processes for the hanging wall and footwall seismogenic zones, which is considered a long-term seismic assessment, after Van Aswegen (2005). Moreover, the size of the seismogenic zone and extent of movement was related to the migration of a significantly sized mining front, reinforcing the view that the large events should be thought of as mine-scale events.

In summary, the characteristics of the seismogenic zones for this case study are as follows:

- Seismogenic zones have significant movement (50 m+) and the rate of movement of seismogenic zones match the advance of mine abutment.
- The middle 80% events in the abutment generally has less than 50 m width.
- The magnitude of the largest events is consistent with the magnitude of other events in the seismogenic zone.
- Seismic source parameters (apparent stress, energy–moment) are consistent with a change in stress across the seismogenic zones.

5 Conclusion

In conclusion, the analysis of stope abutment seismicity at LaRonde mine has provided insights into the nature of mine-scale events and their association with mining-induced stress. The study's use of plane-based TDA has revealed the migration of rock mass failure regions in the mine abutments, with seismic events, including those of significant magnitude, are closely linked to the advancing stoping front.

Apparent stress trends and the energy–moment relation serve to infer rock mass failure characteristics across the yielding region. Events characterised by apparent stress, high energy and low moment in and ahead of the seismogenic region suggest high confinement and minimal deformation of highly stressed rock. This pattern shifts toward lower apparent stress, lower energy and higher moment events in region behind the seismogenic zone, signalling reduced confinement and increased deformation in less stressed rock.

The observed consistency between the magnitudes of the large seismic events and the footwall and hanging wall seismic populations using the Gutenberg-Richter frequency–magnitude relation shows a plausible fit between the mine-scale events and the broader migrating failure region. This supports the hypothesis that these events are part of the same rock mass failure process, which is predominantly stress-induced rather than fault controlled.

As mining extraction increases from greater depths, the occurrence of mine-scale seismic events is likely to remain a substantial risk. The findings of this study underscore the importance of routine seismic data analysis in high stress mining environments. By understanding the behaviour of seismic sources and the seismic hazard associated with them, mining operations can better anticipate and mitigate the risks of large seismic events.

Acknowledgement

Thanks to Marty Hudyma for input and feedback during this investigation and Laura Camball for the comments. Thanks to Agnico Eagle for permission to publish this case study.

References

- Abolfazlzadeh, Y & Hudyma, M 2016, 'Identifying and describing a seismogenic zone in a sublevel caving mine', *Rock Mechanics and Rock Engineering*, vol. 49, pp. 3735–3751.
- Agnico Eagle 2024, LaRonde Complex, <https://www.agnicoeagle.com/English/operations/operations/laronde/maps-and-surveys/default.aspx>
- Aki, K 1966, 'Generation and propagation of G waves from the Niigata earthquake of June 14, 1964, Part 2. Estimation of earthquake moment, released energy and stress-strain drop from G wave spectrum', *Bulletin of the Earthquake Research Institute*, vol. 44, pp. 73–88.
- Amidzic, D 2001, 'Energy-moment relation and its application', in G Van Aswegen, WD Ortlepp & R Durrheim (eds), *Proceedings of the 5th International Symposium on Rockbursts and Seismicity in Mines*, The Southern African Institute of Mining and Metallurgy, Johannesburg, pp. 509–513.
- Boatwright, J 1984, 'Seismic estimates of stress release', *Journal of Geophysical Research*, vol. 89, no. B8, pp. 6961–6968.
- Brune, JN 1970, 'Tectonic stress and the spectra of seismic shear waves from earthquakes', *Journal of Geophysical Research*, vol. 75, no. 26, pp. 4997–5009.
- Counter, D 2014, 'Kidd Mine – dealing with the issues of deep and high stress mining – past, present and future', in M Hudyma & Y Potvin (eds), *Deep Mining 2014: Proceedings from the Seventh International Conference on Deep and High Stress Mining*, Australian Centre for Geomechanics, Perth, pp. 3–22.
- Dineva, S, Dahnér, C, Malovichko, D, Lund, B, Gospodinov, D, Agostinetti, NP & Rudzinski, L 2022, 'Analysis of the magnitude 4.2 seismic event on 18 May 2020 in the Kiirunavaara mine, Sweden', *Proceedings of the Tenth Conference on Rockburst and Seismicity in Mines*, Society for Mining, Metallurgy & Exploration, Englewood.
- Durrheim, RJ, Anderson, RL, Cichowicz, A, Ebrahim-Trollope, R, Hubert, G, Kijko, A, McGarr, A, Ortlepp, WD & Van der Merwe, N 2006, *Investigation into the Risks to Miners, Mines, and the Public Associated with Large Seismic Events in Gold Mining District*, Department of Minerals and Energy, Pretoria
- Earthquakes Canada 2024, 'Earthquake search', Natural Resources Canada, <http://earthquakescanada.nrcan.gc.ca/stndon/NEDB-BNDS/bulletin-en.php>
- Gutenberg, B & Richter, CF 1944, 'Frequency of earthquakes in California', *Bulletin of the Seismological Society of America*, vol. 34, no. 4, pp. 185–188.
- Harris, P & Cumming-Potvin, D 2023, *mXrap*, version 6, Australian Centre for Geomechanics, Perth, mxrap.com

- Hedley, DGF 1992, *Rockburst Handbook for Ontario Hardrock Mines*, CANMET Special Report SP92-1E, Communication Group, Ottawa.
- Heal, D, Hudyma, M & Vezina, F 2005, 'Seismic hazard at Agnico-Eagle's Laronde mine using MS-RAP', *CIM Operators Conference*, Canadian Institute of Mining, Metallurgy and Petroleum, Westmount.
- Hudyma, M, Mikula, P & Heal, D 2003, 'Seismic monitoring in mines – old technology – new applications', *Proceedings of the 1st Australasian Ground Control in Mining Conference*, University of New South Wales School of Mining Engineering, Sydney, pp. 201–218.
- Hudyma, M & Brummer, RK 2006, *Mining induced seismicity review – 2006*, report to Agnico-Eagle Mines Ltd., Itasca Consulting Canada Inc, Vancouver.
- Hudyma, M 2008, *Analysis and Interpretation of Clusters of Seismic Events in Mines*, PhD thesis, The University of Western Australia, Perth.
- Kagan, Y & Knopoff, L 1976, 'Statistical search for non-random features of the seismicity of strong earthquakes', *Physics of the Earth and Planetary Interiors*, vol. 12, no. 4, pp. 291–318.
- Legge, N & Spottiswoode, SM 1987, 'Fracturing and microseismicity ahead of a deep gold mine stope in the pre-remnant and remnant stages of mining', in G Herget & S Vongpaisal (eds), *Proceedings of the 6th International Congress on Rock Mechanics*, Balkema, Rotterdam, pp. 1071–1077.
- Lenhardt, WA 1988, 'Some observations regarding the influence of geology on mining induced seismicity at Western Deep Level', *Proceedings of 1st Regional Conference for Africa – Rock Mechanics in Africa*, South African National Group on Rock Mechanics, Swaziand, pp. 45–48.
- Maeda, K 1999, 'Time distribution of immediate foreshocks obtained by a stacking method', in M Wyss, K Shimazaki & A Ito (eds), *Seismicity Patterns, their Statistical Significance and Physical Meanin*, Birkhäuser, Basel, pp. 381–394.
- Mendecki, A 1993, 'Real time quantitative seismology in mines keynote address', in RP Young (ed.), *Proceedings of the 3rd International Symposium on Rockbursts and Seismicity in Mine*, Balkema, Rotterdam pp. 287–295.
- Mercier-Langevin, F 2010, 'LaRonde extension — mine design at three kilometres', M Van Sint Jan & Y Potvin (eds), *Deep Mining 2010: Proceedings of the Fifth International Seminar on Deep and High Stress Mining*, Australian Centre for Geomechanics, Perth, pp. 3–16.
- Ollila, B 2021, *Time Distance Analysis of a Mine Scale Event*, Msc thesis, Laurentian University, Sudbury.
- Omori, F 1894, 'On the aftershocks of earthquakes', *Journal of the College of Science*, Imperial University of Tokyo, Tokyo, vol. 7, pp. 111–120.
- Ortlepp, WD & Stacey, TR 1994, 'Rockburst mechanisms in tunnels and shafts', *Tunnelling and Underground Space Technology*, vol. 9, no. 1, pp. 59–65.
- Stein, RS 1999, 'The role of stress transfer in earthquake occurrence', *Nature*, vol 402, pp. 605–609.
- Turcotte, P 2010, 'Field behaviour of hybrid bolt at LaRonde Mine', in M Van Sint Jan & Y Potvin (eds), *Deep Mining 2010: Proceedings of the Fifth International Seminar on Deep and High Stress Mining*, Australian Centre for Geomechanics, Perth, pp. 309–320.
- Utsu, T 2002, 'Statistical features of seismicity', in WHK Lee, H Kanamori, PC Jennings & C Kisslinger (eds), *International Geophysics*, Academic Press, Cambridge, pp. 719–732.
- Van Aswegen, G & Butler, A 1993, 'Applications of quantitative seismology in South African gold mines', in RP Young (ed.), *Proceedings of the 3rd International Symposium on Rockbursts and Seismicity in Mines*, Balkema, Rotterdam, pp. 261–266.
- Van Aswegen, G 2005, 'Routine seismic hazard assessment in some South African mines', in Y Potvin & M Hudyma (eds), *Proceedings of the 6th International Symposium on Rockburst and Seismicity in Mines*, Australian Centre for Geomechanics, Perth, pp. 437–444.
- Wesseloo, J, Hudyma, M & Harris, P 2011, 'A community based seismic system for obtaining regional and local seismic data of strategic importance', in Y Potvin (ed.), *Strategic versus Tactical 2011: Proceedings of the Fourth International Seminar on Strategic versus Tactical Approaches in Mining*, Australian Centre for Geomechanics, Perth, pp. 159–168.
- Wesseloo, J 2014, 'Evaluation of the spatial variation of b-value', *Journal of The Southern African Institute of Mining and Metallurgy*, vol. 114, pp. 823–828.

